

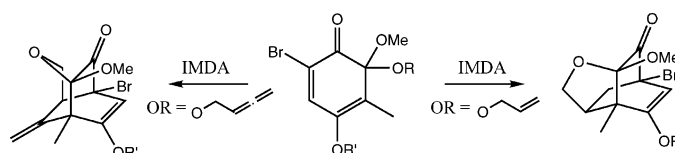
## Characterization of the Switch in the Mechanism of an Intramolecular Diels–Alder Reaction

Carlos Silva López,<sup>\*,†,‡</sup> Olalla Nieto Faza,<sup>†</sup> and Angel R. de Lera<sup>\*,†</sup>

*Departamento de Química Orgánica, Universidade de Vigo, Lagoas Marcosende, 36310 Vigo, Galicia, Spain, and Department of Chemistry, University of Minnesota, 207 Pleasant Street SE, Minneapolis, Minnesota 55455-0431*

*csilval@uvigo.es; qolera@uvigo.es*

*Received September 6, 2007*



Changing the dienophile moiety of an intramolecular Diels–Alder (IMDA) cycloaddition from an allyl ether to an allenyl ether can dramatically change the regioselectivity. We hereby show by density functional theory computations that such unprecedented divergence is produced by an underlying change in the mechanism of the reaction. The allyl ether yields a fused tetrahydrofuran through a classical Diels–Alder reaction, whereas the allenyl ether yields a (methylidene)tetrahydropyran through a stepwise process. The latter reaction involves an extreme asynchronism in the bond-forming events with a diradicaloid intermediate that is stabilized by conjugation and synergistic (captodative) effects. Comparison with intermolecular model D–A reactions, which are concerted processes with various degrees of asynchrony, helps explain the change in regioselectivity for the IMDA reaction of allyl systems and the shift in mechanism for the IMDA reaction of the allenyl derivatives studied.

### 1. Introduction

Very recently, Danishefsky and co-workers reported a powerful complexity-generating sequence to access the central tetracyclic carbon skeleton of the anistatin-related natural product 11-*O*-debenzoyltashironin, a neurotrophically active compound. The one-step process involved the interception of an *o*-quinone dialkylmonoketal (generated by the Tamura–Pelter oxidative dearomatization of phenols in the presence of an unsaturated alcohol) with the pendant unsaturation in an intramolecular Diels–Alder (IMDA) cycloaddition.<sup>1</sup> The IMDA cycloaddition results in the formation of a five-membered ring fused to the [2.2.2] bicyclic skeleton, **2**, or a six-membered ring bridged to the same core unit, **4**, and it was found that the regioselectivity of the IMDA cycloaddition depends only on the carbon type at the dienophile distal position (see Figure 1). The IMDA reaction yields the latter product when this position is occupied by a sp carbon atom and the former in the case of a sp<sup>2</sup> carbon atom. The adduct **2** results from an approach of both reacting units in which the principal functional groups, ketone and ether, are

distal (hereafter denoted as head-to-tail or h–t), and it is the exclusive product with 2,3-propenyl (allyl) ethers. Conversely, the adduct **4** is the consequence of an alternative approach in which both groups are proximal (head-to-head, h–h) and is observed with a 2,3-butadienyl (allenyl) ether as part of the mixed ketal unit. This unexpected experimental finding triggered the need for a modification in the synthetic route; a transannular Diels–Alder reaction was eventually the reaction of choice in the total synthesis of the natural product to the detriment of the intramolecular version to avoid formation of undesired products.<sup>2</sup>

Due to our interest in apparently ill-behaved pericyclic reactions,<sup>3,4</sup> we decided to explore the mechanistic details of this peculiar Diels–Alder cycloaddition in order to determine the electronic and structural features underlying the switch in regioselectivity. Starting from the conclusions Danishefsky and co-workers draw from their experimental findings, we assumed that the key element in this regioselectivity reversal lies in the

(2) Cook, S. P.; Polara, A.; Danishefsky, S. J. *J. Am. Chem. Soc.* **2006**, *128*, 16440–16441.

(3) López, C. S.; Faza, O. N.; de Lera, A. R. *Org. Lett.* **2006**, *8*, 2055–2058.

(4) López, C. S.; Faza, O. N.; Álvarez, R.; de Lera, A. R. *J. Org. Chem.* **2006**, *71*, 4497–4501.

<sup>†</sup> Universidade de Vigo.

<sup>‡</sup> University of Minnesota.

(1) Cook, S. P.; Danishefsky, S. J. *Org. Lett.* **2006**, *8*, 5693–5695.

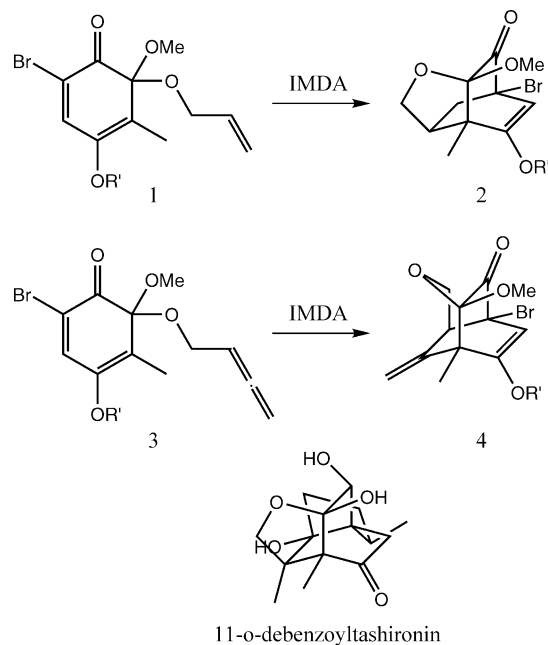


**FIGURE 1.** Intramolecular Diels–Alder in the synthesis of 11-*O*-debenzoyltashironin.

nature of the dienophile and we focused our attention in the differences of vinyl versus allenyl derivatives.

Since the steric hindrance of both an allyl and an allenyl group in the cofacial approach necessary to undergo cycloaddition is very small, cluttering in the transition state seemed an unlikely explanation for such an extreme regioselectivity change. Actually, in line with this hypothesis, Danishefsky and co-workers speculated with the special electronic character of the cumulene carbon atom to justify the selectivity reversal.

## 2. Computational Methods

The density functional theory<sup>5</sup> in its Kohn–Sham<sup>6</sup> formulation was employed throughout this work. All of the stationary points were computed with the three-parameter hybrid functional by Becke in conjunction with the correlation functional by Lee, Yang, and Parr (B3LYP)<sup>7–10</sup> as implemented in Gaussian03.<sup>11</sup> The Pople basis

set was used for C, H, and O atoms, whereas the LanL2DZ relativistic effective core potential and its associated basis set were used for Br.

The choice of DFT and the Pople basis sets is backed by earlier studies in which this method offered reasonable results at a moderate cost despite the presence of diradical species in the reaction profile.<sup>3,12–15</sup>

Due to the potential diradical character of some of the structures considered in this work, the internal and external stabilities of the wavefunctions were computed via the Hermitian stability matrices **A** and **B** in all cases.<sup>16</sup> For all the structures exhibiting unstable restricted wavefunctions, the spin-symmetry constraint of the wavefunction was released (i.e., expanding the SCF calculation to an unrestricted space, UB3LYP), leading to stable unrestricted wavefunctions.

## 3. Results and Discussion

The transition state corresponding to the h–t approach, which leads to the five-membered ring formation, was located for reactants **1** and **3**, furnishing **2** and **4'**, respectively (prime products indicate the nonobserved regioisomer; see Figure 2). These transition states show the characteristic geometry of a Diels–Alder reaction, namely, the cofacial approach in a concerted fashion. The forming bonds display similar lengths (2.2 and 2.4 Å in **TS**<sub>1→2</sub> and 2.2 and 2.3 Å in **TS**<sub>3→4'</sub> for the proximal and distal forming bonds, respectively), and the imaginary frequency associated with the reaction coordinate involves the approach of the diene and dienophile moieties in a highly synchronous motion. The reaction mechanism leading to the six-membered ring formation shows more discrepancies between the allenyl and allyl derivatives. The formation of **4** implies a stepwise process where the h–h approach is highly asynchronous and leads, in an initial stage, to the formation of the distal single bond. A short-lived intermediate with diradical character is thus formed which rapidly collapses to **4** through a low-energy transition state (11.4 kcal/mol). On the other hand, only one transition state could be located for the h–h allyl approach in the pathway from **1** to **2'** which shows signs of the bond formation exclusively at the distal position. Intense work was devoted to locate the transition state related to the bond formation at the allyl proximal position, but all the attempts were unsuccessful.

We have recently reported a theoretical study of the mechanism of a cationic rearrangement<sup>4</sup> described by Trauner and co-workers as the candidate biomimetic reaction in the synthesis of (–)-crispate.<sup>17,18</sup> This reaction, which was initially proposed to be a concerted [ $\pi 4_a + \pi 2_a$ ] Diels–Alder with a tether, was the subject of a careful theoretical examination that concluded that the reaction actually proceeds through just one transition state corresponding to the formation of a single bond, followed by a second barrierless bond formation. The fact that the second

(5) Hohenberg, P.; Kohn, W. *Phys. Rev.* **1964**, *136*, B864–B871.

(6) Kohn, W.; Sham, L. *Phys. Rev. A* **1965**, *140*, A1133–A1138.

(7) Becke, A. D. *Phys. Rev. A* **1988**, *38*, 3098–3100.

(8) Becke, A. D. *J. Chem. Phys.* **1993**, *98*, 5648–5652.

(9) Stephens, P. J.; Devlin, F. J.; Chabalowski, C. F.; Frisch, M. J. *J. Phys. Chem.* **1994**, *98*, 11623–116237.

(10) Lee, C.; Yang, W.; Parr, R. G. *Phys. Rev. B* **1988**, *37*, 785–789.

(11) Frisch, M. J.; Trucks, G. W.; Schlegel, H. B.; Scuseria, G. E.; Robb, M. A.; Cheeseman, J. R.; Montgomery, J. A., Jr.; Vreven, T.; Kudin, K. N.; Burant, J. C.; Millam, J. M.; Iyengar, S. S.; Tomasi, J.; Barone, V.; Mennucci, B.; Cossi, M.; Scalmani, G.; Rega, N.; Petersson, G. A.; Nakatsuji, H.; Hada, M.; Ehara, M.; Toyota, K.; Fukuda, R.; Hasegawa, J.; Ishida, M.; Nakajima, T.; Honda, Y.; Kitao, O.; Nakai, H.; Klene, M.; Li, X.; Knox, J. E.; Hratchian, H. P.; Cross, J. B.; Bakken, V.; Adamo, C.; Jaramillo, J.; Gomperts, R.; Stratmann, R. E.; Yazyev, O.; Austin, A. J.; Cammi, R.; Pomelli, C.; Ochterski, J. W.; Ayala, P. Y.; Morokuma, K.; Voth, G. A.; Salvador, P.; Dannenberg, J. J.; Zakrzewski, V. G.; Dapprich, S.; Daniels, A. D.; Strain, M. C.; Farkas, O.; Malick, D. K.; Rabuck, A. D.; Raghavachari, K.; Foresman, J. B.; Ortiz, J. V.; Cui, Q.; Baboul, A. G.; Clifford, S.; Cioslowski, J.; Stefanov, B. B.; Liu, G.; Liashenko, A.; Piskorz, P.; Komaromi, I.; Martin, R. L.; Fox, D. J.; Keith, T.; Al-Laham, M. A.; Peng, C. Y.; Nanayakkara, A.; Challacombe, M.; Gill, P. M. W.; Johnson, B.; Chen, W.; Wong, M. W.; Gonzalez, C.; Pople, J. A. *Gaussian 03*, revision C.02; Gaussian, Inc.: Wallingford, CT, 2004.

(12) Hess, B. A., Jr.; Eckart, U.; Fabian, J. *J. Am. Chem. Soc.* **1998**, *120*, 12310–12315.

(13) Hess, B. A., Jr.; Smentek, L.; Brash, A. R.; Cha, J. K. *J. Am. Chem. Soc.* **1999**, *121*, 5603–5604.

(14) López, C. S.; Faza, O. N.; York, D. M.; de Lera, A. *J. Org. Chem.* **2004**, *69*, 3635–3644.

(15) López, C. S.; Faza, O. N.; de Lera, A. R. *Chem.–Eur. J.* **2007**, *13*, 5009–5017.

(16) Bauernschmitt, R.; Ahlrichs, R. *J. Chem. Phys.* **1996**, *22*, 9047–9052.

(17) Miller, A. K.; Banghart, M. R.; Beaudry, C. M.; Suh, J. M.; Trauner, D. *Tetrahedron* **2003**, *59*, 8919–8930.

(18) Miller, A. K.; Byun, D. H.; Beaudry, C. M.; Trauner, D. *Proc. Natl. Acad. Sci. U.S.A.* **2004**, *101*, 12019–12023.

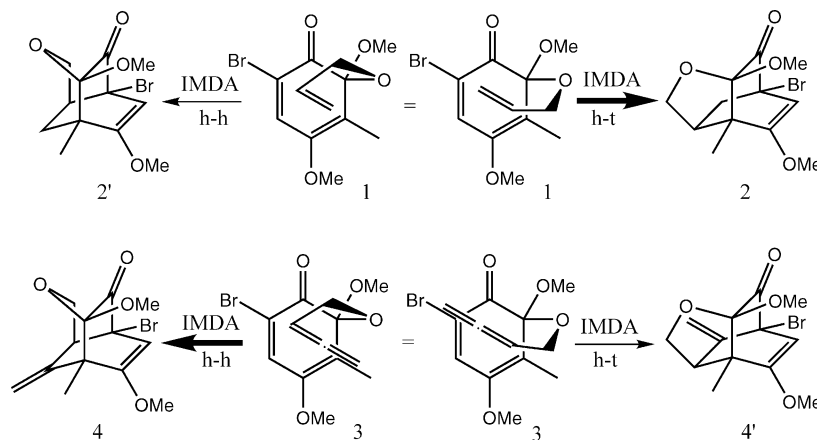


**FIGURE 2.** Proposed cofacial approximations and corresponding adducts for the IMDA cycloaddition of **1** and **3**.

step is barrierless implies that only one transition state is to be found along the reaction coordinate and two bond-forming stages can be defined.

This precedent prompted us to carry out a comprehensive analysis of the potential energy surface for the h–h approach of the allyl and allenyl derivatives. The two bond lengths involved in the putative six-membered cycloaddition process were scanned for the reactions **1** → **2'** and **3** → **4**. A grid of 21 × 21 points, covering the length range of 1.4–3.4 Å, was used, totaling 441 partial geometry optimizations for each reaction. The 2D potential energy surfaces thus obtained are illustrated in Figure 3. The key mechanistic steps in the two surfaces can be summarized as follows. (1) Allyl derivative **1** → **2'** (only one transition state, no intermediates involved): (step i) Single bond formation at the distal site, involving the only TS in the potential energy surface. (step ii) Downhill switch in the reaction coordinate to yield a diradicaloid structure. No intermediate is involved in this change. (step iii) Barrierless collapse of the diradicaloid forms the proximal C–C bond. (2) Allenyl derivative **3** → **4** (two transition states, one intermediate): (step i) Single bond formation at the distal site results in a diradicaloid intermediate. (step ii) Collapse of the diradical via a low-energy transition state, forming the bond at the proximal site in the bicyclic intermediate.

Inspection of Table 1 and Figure 3 helps to understand the mechanistic details in this anomalous IMDA reaction. The fact that for both allyl and allenyl ethers the h–h dienophile approach involves an early transition state, where only the distal C–C bond is formed, is noteworthy. Moreover, this early transition state is rate-limiting regardless of the presence of an intermediate (see Table 1). Actually, from a qualitative point of view, both two-dimensional potential energy surfaces are very similar, with the only exception being an additional stabilization in the region where the reaction coordinate switches in the case of allenyl ether **3**. In this latter mechanism, the intermediate **int** is, in fact, the key to understanding the unexpected change in regioselectivity. Intermediate **int** provides a convenient low-energy stationary point along the reaction path where the switch in the reaction coordinate can occur at a very small expense in energy. This is because **int** exhibits a remarkable set of structural properties that allows two separate radical systems to lie in stable

conjugated  $\pi$  environments.<sup>19</sup> On the one hand, **int** contains a radical delocalized over an allylic  $\pi$  system (the estimated stabilization of an allyl radical due to allylic resonance is 14.2 kcal/mol at the MP4(SDTQ)/6-311G(d,p)//MP2/6-31G(d,p) level),<sup>20</sup> and on the other hand, it also contains an unsaturated 1,4-keto-enolic system that can host a second radical which is stabilized via a synergistic push–pull electronic entanglement (also called captodative effects or merostabilization;<sup>21</sup> see Figure 4). The diradical stabilization due to captodative effects was estimated by considering the energy difference of a model allyl radical and the nonconjugated perpendicular 3-propenyl structure, following the same recipe Seetula employed to estimate the allylic stabilization by resonance (see Figure 5).<sup>20</sup> A captodative stabilization of 7.1 kcal/mol was obtained through these calculations at the B3LYP/6-31G(d,p) level, a remarkable effect that can very well account for the occurrence of a shallow intermediate.

Structural parameters of the transition states and the only intermediate found for this set of four reaction pathways also help to understand key differences and similarities between the allyl and allenyl derivatives (see Figure 6). Structurally both h–t and h–h are very similar, with h–t presenting a slightly asynchronous transition state, whereas the bond lengths of the h–h counterparts are severely asymmetrical (ca. 2 vs 3 Å). The reaction profile in this latter case can be rationalized by means of the FMO theory: a strongly stabilizing secondary interaction in the transition state occurs between the radical-supporting orbitals that leads to a barrierless bond formation downhill from the only transition state (where the first bond is formed). This kind of rationale has been used in other cases of nonconventional potential energy surfaces where dynamic effects have to be considered to explain the reaction kinetics.<sup>22</sup>

In order to provide a deeper insight into the sources of this peculiar reactivity, we have also considered the study of model intermolecular Diels–Alder reactions. Key features of both the diene and dienophile moieties in the IMDA reaction were

(19) The  $\langle S^2 \rangle$  value of **int** is 0.96 before annihilation and 0.28 after annihilation of the triplet contribution; both values are fairly large and qualitatively suggest a strong diradical character for this intermediate. This conclusion is in good agreement with the spin density illustrated in Figure 4.

(20) Seetula, J. A. *Phys. Chem. Chem. Phys.* **1999**, *1*, 4727–4731.

(21) Bordwell, F. G.; Lynch, T.-Y. *J. Am. Chem. Soc.* **1989**, *111*, 7558–7562.

(22) Ussing, B. R.; Hang, C.; Singleton, D. A. *J. Am. Chem. Soc.* **2006**, *128*, 7594–7607.

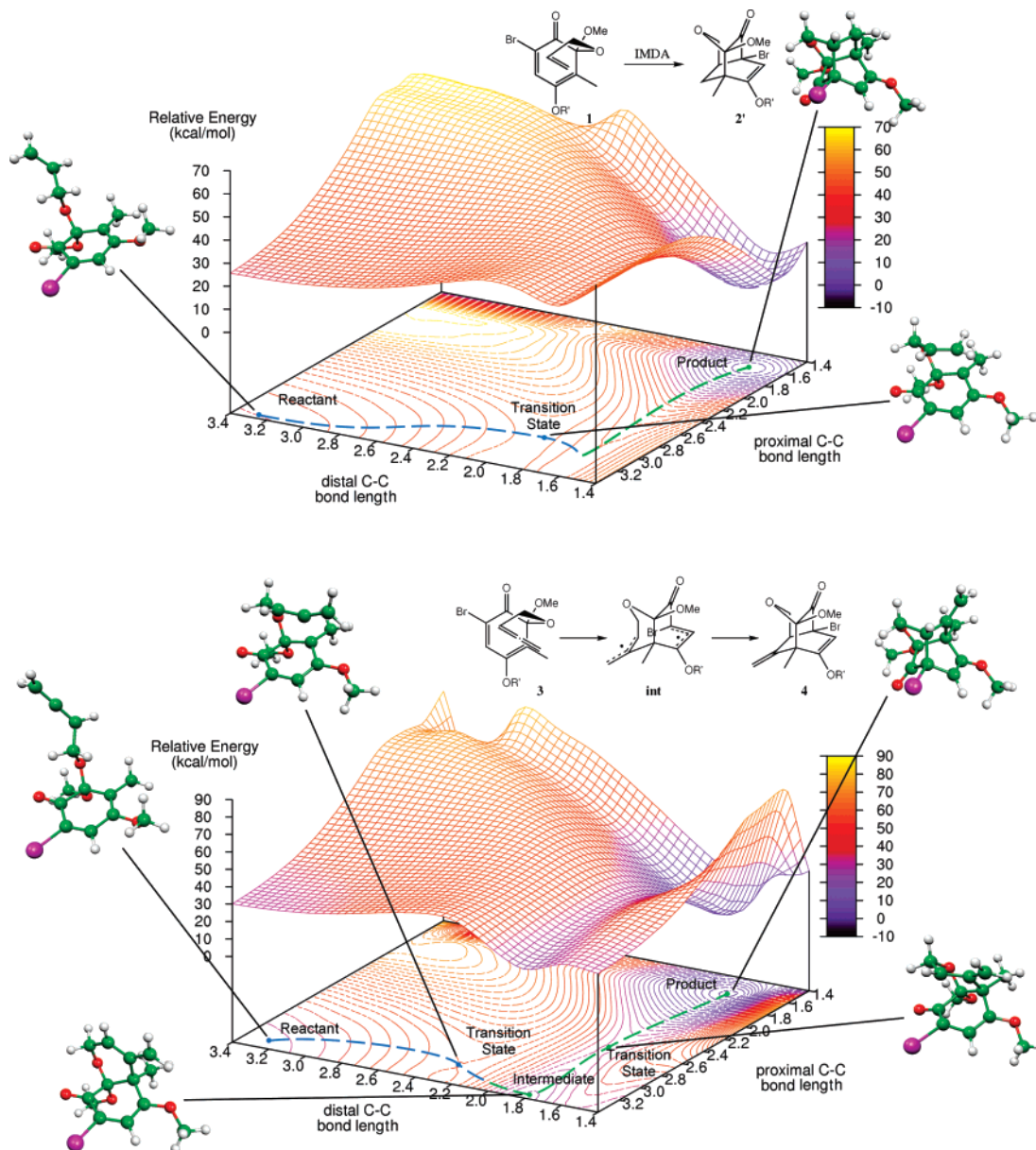


**FIGURE 3.** Two-dimensional potential energy surface for the formation of **2'** from **1** (top) and **4** from **3** (bottom). Relative energies are scaled with respect to each final product. The reaction path is shown with a dashed line on the contour surface projected onto the bottom of the plot. Green color indicates the diradicaloid collapse step.

deemed to be preserved by appropriate functional group substitutions. A ring-strain-free dioxolane replaced the mixed ketal in the diene to avoid artificial steric cluttering and conformational freedom, whereas a methyl group was included in the dienophile ether in lieu of the cyclic counterparts **1** and **3**. We did not consider other approaches of the diene and the dienophile that provide diastereomers of the final product since they are irrelevant to the IMDA mechanism (see Figure 7).

Interestingly, the intermolecular reactions do not seem to be as largely affected by the cumulene atom as the IMDA reactions are. First, a single transition state, responsible for the formation of both new single bonds in the final adduct, is found along the reaction coordinate for all four bimolecular transition states under consideration. Second, the relative energies between the h-h and h-t approaches are similar for both the allyl and the allenyl cycloadditions. Third, the forming bond lengths are also very similar in both the allyl ether and the allenyl ether (see

**TABLE 1.** Thermodynamic Data for the IMDA Reactions of **1** and **3**<sup>a</sup>

<b>1</b> → <b>2</b>			<b>1</b> → <b>2'</b>		
	$\Delta H$	$\Delta G$		$\Delta H$	$\Delta G$
<b>1</b>	0.0	0.0	<b>1</b>	0.0	0.0
<b>TS</b> <sub>1→2</sub>	20.2	24.5	<b>TS</b> <sub>1→2'</sub>	21.1	26.1
<b>2</b>	-26.5	-20.9	<b>2'</b>	-19.0	-12.8
<b>3</b> → <b>4</b>			<b>3</b> → <b>4'</b>		
	$\Delta H$	$\Delta G$		$\Delta H$	$\Delta G$
<b>3</b>	0.0	0.0	<b>3</b>	0.0	0.0
<b>TS</b> <sub>3→int</sub>	17.9	22.8	<b>TS</b> <sub>3→4'</sub>	22.7	27.5
<b>int</b>	-5.3	-0.3	<b>4'</b>	-32.9	-26.8
<b>TS</b> <sub>int→4</sub>	4.1	11.1			
<b>4</b>	-26.3	-20.0			

<sup>a</sup> Relative enthalpies and free energies (in kcal/mol, 298.15 K) computed at the B3LYP/6-31G(d,p) level for the IMDA reactions shown in Figure 2.

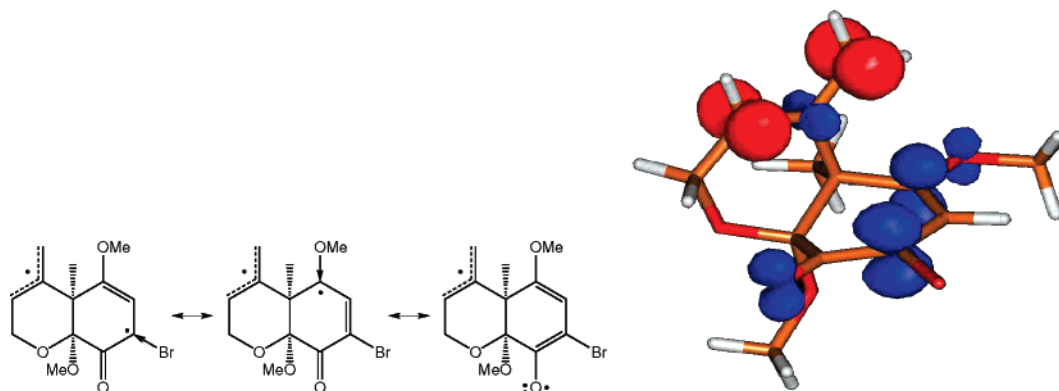


**FIGURE 4.** Spin density (0.01 au isosurface) of intermediate **int**. In the scheme, the main resonance forms for the diradical species are shown as a qualitative explanation. They correctly predict the radical delocalization in two separate systems: an allyl radical and the 1,4-keto-enolic system with stabilizing donor substituents in the appropriate positions.

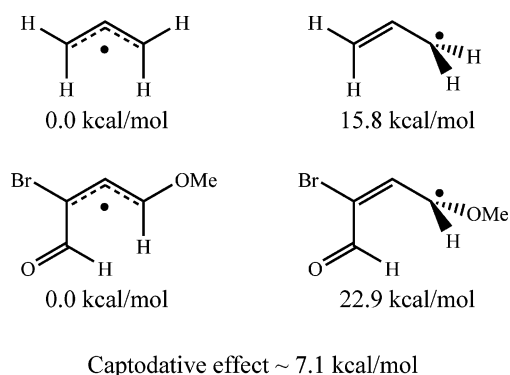


**FIGURE 5.** Relative free-energy values (B3LYP/6-31G(d,p) level) of model systems to estimate the stabilization of **int** (Figure 4) due to captodative effects.

Figure 7 and Table 2). From these intermolecular transition states, it is clear that the regioselectivity is reversed in the allyl derivative by the inclusion of the tether in the IMDA reaction. The tether also changes the mechanism of the allenyl (vide infra) counterpart, although the regioselectivity is not reversed in this case. In the intermolecular model reaction, both the allyl and the allenyl derivatives present a lower-energy transition state for the h–h regioisomer ( $TS_{1\rightarrow 2}^{inter}$  and  $TS_{3\rightarrow 4}^{inter}$ ), whereas in the IMDA reaction, the allyl ether **1** yields the five-membered ring adduct **2** through the h–t approach. These low-energy intermolecular transition states exhibit a considerable degree of asynchronism (forming bond lengths of ca. 2.1 and 2.8 Å), but the transition state is still concerted and the normal mode with an imaginary frequency associated with the cycloaddition reaction shows evidence of bond formation at both ends of the diene. The high-energy intermolecular transition states ( $TS_{1\rightarrow 2}^{inter}$  and  $TS_{3\rightarrow 4}^{inter}$ ), related to the h–t regioisomers, exhibit a very synchronous bond-forming structure, in line with the academic ethylene + butadiene example of a Diels–Alder reaction.

It can be thus concluded that the main effect the allenyl group causes on the intermolecular mechanism is a strong desynchronization at the transition state. Concertedness is nevertheless unaffected by the cumulene carbon, and the cycloaddition occurs through only one transition state. This effect is further boosted by the inclusion of the tether, which introduces a ring-strain term in the total energy, displacing

the transition states more toward asynchrony. Taking into account the ability of allene groups to stabilize radicaloid species through conjugation, it seems clear that the synergistic effects of the allene and the tether drive the IMDA reaction toward such an extreme degree of asynchrony that results in a complete separation of the bond-forming events. The energy penalty associated with the packed Diels–Alder transition state is thereby spread along two single bond-forming steps, a distal C–C bond formation and a subsequent diradical collapse to yield the final adduct. The allene stabilization is also large enough to allow for the location of an intermediate in an otherwise typically concerted process.

A growing number of reactions are being discovered whose mechanistic profiles defy the academic dichotomy between concerted and stepwise processes. Parallel to this shady area in the reaction mechanism lies a confusing lack of consensus in terminology, with interesting proposals for classifying categories that lack, however, widespread acceptance. Terms such as *twixtyl*<sup>23</sup> or *caldera*<sup>24</sup> formulated by Hoffmann and von E. Doering, respectively, could be an adequate patch for this terminology gap in certain cases, but their applicability is not general enough to make them the categories of choice. *Twixtyl*, for example, defines a plateau in which single bond rotation can happen, as it would in a conventional intermediate characterized by a well in the PES; however, this is not a common feature of plateau species.<sup>4,25,26</sup> The related Doering's *caldera*, “a ‘diradical’ transition region characterized as a relatively ‘flat’, multidimensional, free energy surface”, is a term inherently associated with diradicals and thus lacks generality in a world where plateaus in molecular potential energy surfaces can also be found for closed-shell systems.<sup>26–28</sup>

(23) Hoffmann, R.; Swaminathan, S.; Odell, B. G.; Gleiter, R. *J. Am. Chem. Soc.* **1970**, *92*, 7091–7097.

(24) von E. Doering, W.; Ekmanis, J. L.; Belfield, K. D.; Klärner, F.-G.; Krawczyk, B. *J. Am. Chem. Soc.* **2001**, *123*, 5532–5541.

(25) Singleton, D. A.; Hang, C.; Szymanski, M. J.; Greenwald, E. E. *J. Am. Chem. Soc.* **2003**, *125*, 1176–1177.

(26) Singleton, D. A.; Hang, C.; Szymanski, M. J.; Meyer, M. P.; Leach, A. G.; Kuwata, K. T.; Chen, J. S.; Greer, A.; Foote, C. S.; Houk, K. N. *J. Am. Chem. Soc.* **2003**, *125*, 1319–1328.

(27) Bartsch, R. A.; Chae, Y. M.; Ham, S.; Birney, D. M. *J. Am. Chem. Soc.* **2001**, *123*, 7479–7486.

(28) González-Lafont, A.; Moreno, M.; Lluch, J. M. *J. Am. Chem. Soc.* **2004**, *126*, 13089–13094.

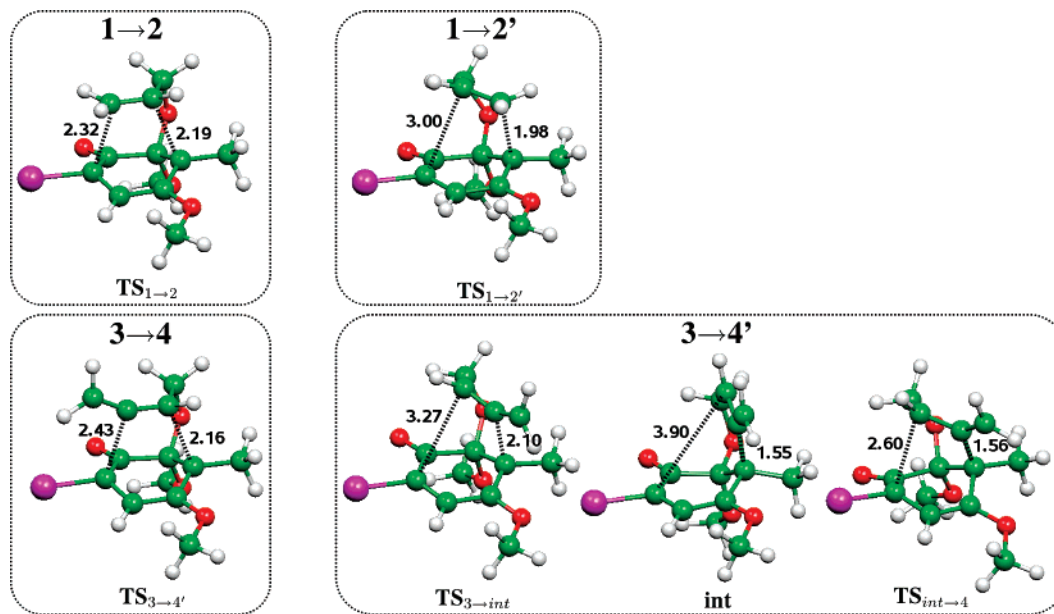


FIGURE 6. Bond lengths of the transition states and intermediate involved in the transformations of **1** and **3**.

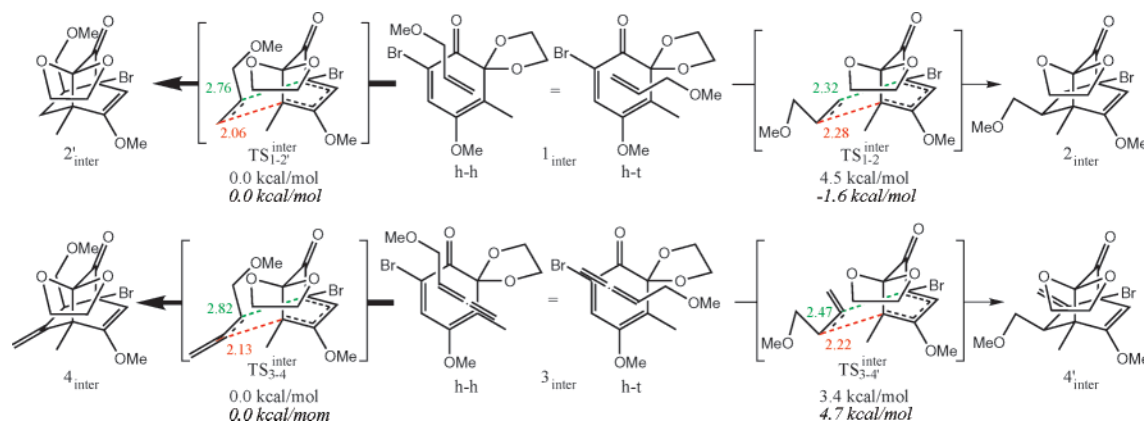


FIGURE 7. Transition states for intermolecular DA reaction mimicking the **1** → **2** ( $TS_{1-2}^{inter}$ ), **1** → **2'** ( $TS_{1-2'}^{inter}$ ), **3** → **4** ( $TS_{3-4}^{inter}$ ), and **3** → **4'** ( $TS_{3-4'}^{inter}$ ) IMDA reactions shown in Figure 2. Shown are forming bond lengths (Å) and relative free energies (kcal/mol). For comparison, relative free activation energies of the rate-limiting step for the modeled intramolecular reactions are also shown in italics.

TABLE 2. Thermodynamic Data for the Model Intermolecular Reactions Illustrated in Figure 7<sup>a</sup>

$1_{inter} \rightarrow 2_{inter}$		$1_{inter} \rightarrow 2'_{inter}$	
$\Delta H$	$\Delta G$	$\Delta H$	$\Delta G$
<b>1</b> <sub>inter</sub>	0.0	<b>1</b> <sub>inter</sub>	0.0
<b>TS</b> <sub>1-2</sub> <sup>inter</sup>	22.7	<b>TS</b> <sub>1-2'</sub> <sup>inter</sup>	17.5
<b>2</b> <sub>inter</sub>	-26.6	<b>2'</b> <sub>inter</sub>	-25.8
$3_{inter} \rightarrow 4_{inter}$		$3_{inter} \rightarrow 4'_{inter}$	
$\Delta H$	$\Delta G$	$\Delta H$	$\Delta G$
<b>3</b> <sub>inter</sub>	0.0	<b>3</b> <sub>inter</sub>	0.0
<b>TS</b> <sub>3-4</sub> <sup>inter</sup>	20.9	<b>TS</b> <sub>3-4'</sub> <sup>inter</sup>	23.9
<b>4</b> <sub>inter</sub>	-35.6	<b>4'</b> <sub>inter</sub>	-31.8

<sup>a</sup> Relative enthalpies and free energies (in kcal/mol, 298.15 K) computed at the B3LYP/6-31G(d,p) level of theory.

#### 4. Conclusion

Intramolecular D–A cycloadditions of systems related to those used by Danishefsky and co-workers for the synthesis of 11-*O*-debenzoyltashironin are shown to differ from the corre-

sponding intermolecular counterparts both in regioselectivity (allyl ether tether) and mechanism (allenyl ether tether). Whereas the IMDA reaction of the former shows features of a concerted but considerably asynchronous D–A reaction, the IMDA reaction of the latter is best described as a stepwise reaction with a diradical intermediate. The systems under study seem to belong to a group of reactions in a frontier where the textbook dichotomy between concerted and stepwise mechanisms is insufficient. A minor structural change in these cases leads to one side of the border or the other. This frontier can be understood considering a formal two-step reaction in which the second step is a barrierless process. In these conditions, no intermediate can be expected between the two steps, but still, they are clearly differentiated and the reaction coordinate is drastically different at the initial and final stages of the bond-breaking/forming events. Under these premises, neither a concerted nor a stepwise mechanism is a suitable description of the reaction. We have hereby shown that a more subtle and thorough analysis must be conducted in such cases.

**Acknowledgment.** The authors are grateful to the Xunta de Galicia (Parga Pondal Contract to C.S.L.) and the Spanish Ministerio de Educación y Ciencia (SAF04-07131, FEDER) for financial support, and the MSI and CESGA for generous allocation of computing resources.

**Supporting Information Available:** Cartesian coordinates, SCF energies, and the number of imaginary frequencies for all the computed structures. This material is available free of charge via the Internet at <http://pubs.acs.org>.

JO701962T